CHEM. RES. CHINESE UNIVERSITIES
2008, 24(1), 96—100
Article ID 1005-9040(2008)-01-096-05

Kinetics and Mechanism of the Photo-oxidation of Thiophene by O_2 Adsorbed on Molecular Sieves

ZHAO Di-shun[1,2*], LI Fa-tang[2,3], ZHOU Er-peng[2] and SUN Zhi-min[3]

1. College of Chemical and Pharmaceutical Engineering, Hebei University of Science and Technology, Shijiazhuang 050018, P. R. China;

2. School of Chemical Engineering, Tianjin University, Tianjin 300072, P. R. China;

3. College of Science, Hebei University of Science and Technology, Shijiazhuang 050018, P. R. China

Abstract Photochemical oxidation of thiophene in *n*-octane/water extraction system using O_2 as oxidant was studied. The reaction mechanism of thiophene oxidation was proposed. Results obtained here can be used as the reference for the oxidative desulfurization of gasoline because thiophene is one of the main components containing sulfur in fluid catalytic cracking gasoline. Thiophene dissolved in *n*-octane was photodecomposed and removed into the water phase at ambient temperature and atmospheric pressure. A 500 W high-pressure mercury lamp (main wave length 365 nm, 0.22 kW/m) was used as light source for irradiation, and air was introduced by a gas pump to supply O_2. Thiophene can be photo-oxidized to sulfone, oxalic acid, SO_4^{2-}, and CO_2. The desulfurization yield of thiophene in *n*-octane is 58.9% under photo-irradiation for 5 h under the conditions of air flow at 150 mL/min and V(water):V(*n*-octane)=1:1. It can be improved to 92.3% by adding 0.15 g zeoliteartificial into 100 mL reaction system, which is the adsorbent for O_2 and thiophene. And under such conditions, the photo-oxidation kinetics of thiophene with O_2/zeoliteartificial is first-order with an apparent rate constant of 0.5047 h^{-1} and a half-time of 1.37 h. The sulfur content can be depressed from 800 μL/L to less than 62 μL/L.

Keywords Thiophene; Desulfurization; Photo-oxidation kinetics; Mechanism; Photo-oxidation product; Molecular sieve

1 Introduction

During the combustion of fuels, SO_x is emitted, which is one of the main sources of acid rain and air pollution. To protect environment against contamination, legislation has limited the sulfur content in light oil to maximum 50 mg/L in Europe in 2005. The United States also has limited that for highway use to 15 mg/L by June 2006[1].

Catalytic hydrodesulfurization is commonly used to decrease the sulfur content in oil. Desulfurization is generally conducted at a high pressure (>5 MPa) and at a high temperature (>520 K) by the reaction of hydrogen gas with sulfur compounds in the presence of catalyst[2]. However, it is difficult to meet the demand of deep desulfurization(<50 mg/L) because dibenzothiophenes(DBTs) are highly resistant to hydrogenation and require the use of modified catalyst and more severe reaction conditions[3]. An alternative process, able to be operated under moderate conditions in the absence of H_2 and catalyst, is therefore urgently required.

Photochemical oxidation is a novel technique to degrade sulfur-containing compounds in oil and has received much attention for the deep desulfurization of light oil in recent years[4,5]. In these reactions, the process is comprised of two stages. The first stage consists of the transfer of sulfur-containing compounds in light oil to a polar extraction solvent. It is then followed by the photo-oxidation and photodecomposition of sulfur-containing compounds by UV irradiation[6—8].

Thiophenes, benzothiophenes, and dibenzothiophenes are the main sulfur-containing compounds in light oil[9], and the study on their desulfurization is necessary to guide the desulfurization of oil. There have been reports about the photochemical oxidation of benzothiophenes and dibenzothiophenes[10—12] and also about the oxidative desulfurization of thiophenes[13]. But there have been only few reports concerning the mechanism of photo-oxidation and the products of thiophenes.

* Corresponding author.. E-mail: gzlun418@yahoo.com.cn

Received March 16, 2007; accepted May 12, 2007.

Supported by the Science and Technology Development Planning Foundation of Jilin Province, China(No.20030405).

In our previous study[14], the mechanism of photo-oxidation and products of thiohpene by O_2 in *n*-octane/water extraction system was briefly proposed. But the dissolved content of O_2 in water is low, so the desulfurization yield is limited. To improve the desulfurization yield, different molecular sieves were added into system as adsorbents for O_2 in this article. And the effects of addition of molecular sieves on the desulfurization of thiophene were also investigated.

2 Experimental

2.1 Materials

Thiophene(99%) was purchased from Johnson Matthey Co. MeCN, *n*-octane, $KMnO_4$, $BaCl_2$, zeoliteartificial(20—40 mesh), and molecular sieves were of analytical grade and were used as received. The photo-oxidation reaction was conducted in an XPA-II photochemical reactor as shown in Fig.1, which was produced by Nanjing Xujiang Electromechanical Factory.

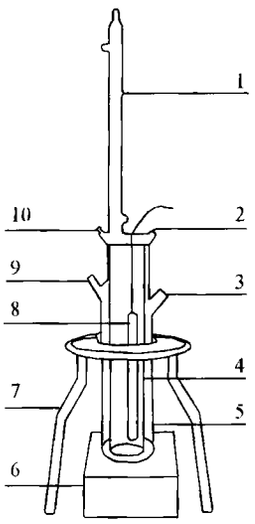

Fig.1 Schematic diagram of experimental apparatus

1. Condenser; 2. inlet of water; 3. inlet of air; 4. silicon cold trap; 5. glass reactor; 6. magnetic stirrer; 7. bracket of reactor; 8. Hg lamp; 9. outlet of air; 10. outlet of water.

2.2 Procedure

A total of 0.106 mL thiophene was dissolved in *n*-octane(50 mL) to form model gasoline, the sulfur content of which was 800 μL/L and mixed vigorously with water(25—150 mL). The combined solution was UV irradiated using a high-pressure mercury lamp(500 W, main wave length 365 nm, 0.22 kW/m^2). During photoirradiation, air was introduced by a gas pump to dissolve O_2 in the water solution. And the air coming out of the outlet was introduced into distilled water or a $Ca(OH)_2$ solution, the pH of which was measured by a pH meter(Mettler Toledo, Delta 320). To determine the initial and residual sulfur contents in the organic phase, liquid samples were withdrawn from the reactor at fixed time intervals and measured using a micro coulometer(WK-2D, Jiangsu Jiangfen Electroanalysis Company Limited) and then desulfurization yield was calculated. The products of thiophene after photo-oxidation was analyzed using Fourier Transform Infrared Spectroscopy(FTIR, Shimadzu IRPRESTIGE-21), MeCN was used as the extraction phase to replace water. To observe the GC peak before and after reaction, the organic phase was analyzed using a gas chromatograph equipped with FPD on a SE-30 column of φ 0.32 mm×30 m(7890, Shanghai Tianmei Experiment Company Limited). The main parameters were as follow: oven temperature 120 °C, injector temperature 160 °C, detector temperature 170 °C and 0.2 μL of sample was injected.

3 Results and Discussion

3.1 Influence of Air Flow on Desulfurization Yield of Model Gasoline

The influence of air flow on the desulfurization yield of model gasoline is shown in Table 1 after photoirradiation for 5 h in the system with V(water): V(*n*-octane)=1:1.

Table 1 Influence of air flow on the desulfurization yield of thiophene

Air flow/(mL·min^{-1})	0	50	100	150	200	300
Desulfurization yield(%)	10.2	35.2	48.9	58.9	53.5	46.3

It was also found that the desulfurization yield of model gasoline could reach 7.8% after the mixing of the combined solutions for 2 min without photoirradiation and the introduction of air. The result indicates that some polar thiophene was transferred into water phase from nonpolar *n*-octane. In water phase, thiophene was successfully oxidized by O_2 under photoirradiation to form highly polarized compounds, which were not distributed into the nonpolar *n*-octane phase. When *n*-octane and water were mixed and photoirradiated, thiophene was successively extracted and photooxidized in the water phase.

When air was not introduced, the desulfurization yield of model gasoline was 10.2%. The reason was that thiophene was oxidized by O_2 dissolved in water,

and thiophene itself could not be degraded by photoirradiation only. And it could be seen that the desulfurization yield increased with air flow at first and reached the highest with air flow at 150 mL/min because of the increase of $^1O_2$ obtained by the excitation of O_2, which was the oxidant for thiophene excited by O_2. When the rate of air flow was above 150 Ml/min, the desulfurization yield decreased because of the extra volatilization of *n*-octane. And the desulfurization yield of model gasoline was 5.1% after 5 h at an air flow rate of 150 mL/min and without photoirrigation, the reason was that the volatilization of *n*-octane was faster than that of thiophene.

3.2 Influence of Water/*n*-Octane Volume Ratio on Desulfurization Yield of Model Gasoline

The desulfurization yields of thiophene in *n*-octane are shown in Table 2 after photoirradiation for 5 h at an air flow rate of 150 mL/min.

Table 2 Influence of volume ratio of MeCN/*n*-octane on the desulfurization yield of thiophene

V(water)/*V*(*n*-octane)	0.5:1	1:1	1.5:1	2:1	3:1
Desulfurization yield(%)	49.3	58.9	57.8	46.3	40.9

As shown in Table 2, the desulfurization yield of model gasoline increased with the increase in water/*n*-octane volume ratio at first. When the volume ratio of water/*n*-octane was low, the extraction effect of water for model gasoline was bad. When the volume ratio of water/*n*-octane was too high, the contiguity effect under water phase and above *n*-octane phase decreased because of the stirring.

3.3 Influence of the Amount of Molecular Sieves on the Desulfurization Yield of Model Gasoline

As the solubility of O_2 in water solution was limited, thiophene in *n*-octane phase could not be oxidized by enough O_2. To improve the desulfurization yield of model gasoline, different molecular sieves(3A, 4A, and 5A) were added into the two-phase system as adsorbents for O_2 to increase the solubility of O_2 in water. The experimental results are shown in Fig.2.

The molecular sizes of O_2 and N_2 in air are 0.38 nm×0.28 nm and 0.42 nm×0.30 nm, respectively, and the pore diameter of 3A, 4A, and 5A molecular sieves are 0.30, 0.42, and 0.48 nm, respectively. That is, O_2 and N_2 could not be adsorbed into the pores of 3A molecular sieve and only adsorbed onto the surface of 3A molecular sieve. And N_2 could be adsorbed into the pores of 5A molecular sieve, whereas it restricted the

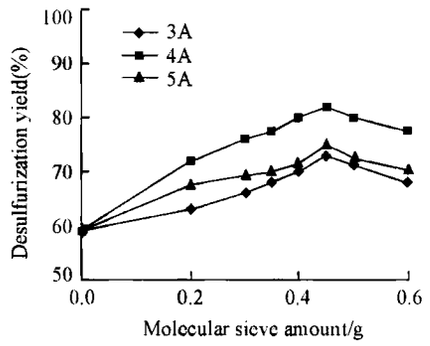

Fig.2 Effects of different molecular sieves on the desulfurization yield of thiophene in *n*-octane

Reaction conditions: $V(H_2O):V(n\text{-octane})=1:1$; air flow 150 mL/min.

adsorption of O_2. 4A molecular sieve was the perfect adsorption material of O_2 because of its appropriate pore size. Appropriate amounts of addition of molecular sieves into the system could improve desulfurization yield. The addition of more molecular sieve decreased the desulfurization yield because the molecular sieve scattered UV in the solution and facilitate the absorption of O_2 and thiophene to UV light.

If thiophene could be adsorbed into the molecular sieve, the desulfurization yield would increase. The molecular size of thiophene was 0.55 nm×0.41 nm×0.20 nm[15], which was bigger compared with all other molecular sieves. Zeoliteartificial with the pore diameter of 1.0 nm was used as the adsorbent for thiophene and O_2. The results are shown in Fig.3.

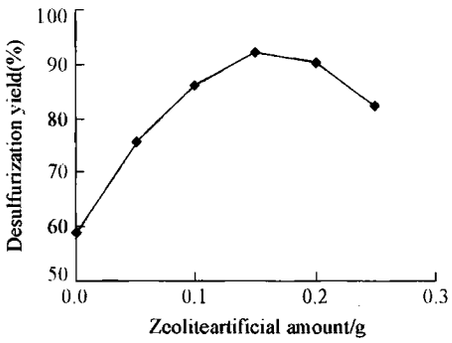

Fig.3 Effect of the addition of zeoliteartificial on the desulfurization yield of thiophene in *n*-octane

Reaction conditions: $V(H_2O):V(n\text{-octane})=1:1$; air flow 150 mL/min.

It could be seen from Fig.3 that the desulfurization yield of thiophene was up to 92.3% when 0.15 g zeoliteartificial was added into the system after photoirradiation for 5 h, which was higher than 82%, which is the desulfurization yield of thiophene with

the addition of 0.45 g of 4A molecular sieve.

3.4 Photo-oxidation Kinetics of Thiophene

To study the photo-oxidation kinetics of thiophene, samples(0.5 mL) were taken out at set time intervals of 0.5 h from *n*-octane phase and measured using a micro coulometer to determine sulfur content in each reaction course. The results are shown in Fig. 4.

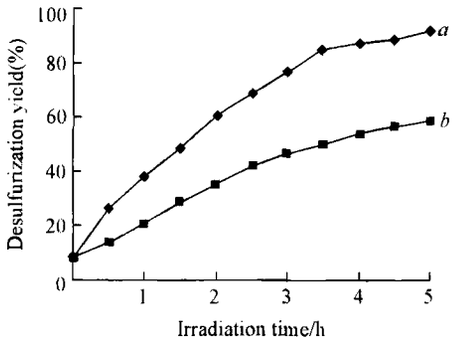

Fig.4 Time-course variation of desulfurization yield of thiophene in *n*-octane

Reaction conditions: $V(H_2O):V(n\text{-octane})=1:1$; air flow 150 mL/min. *a*. 0.15 g zeoliteartificial.

Fig.5 shows the gas chromatogram of thiophene in *n*-octane before and after photo-oxidation.

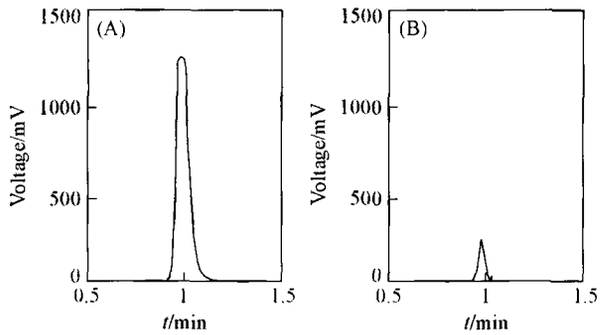

Fig.5 GC-FPD chromatogram of thiophene in *n*-octane before(A) and after(B) reaction(0.15 g zeoliteartificial added)

When the photo-oxidation of thiophene by O_2 follow first-order kinetics, the sulfur content of model gasoline would meet the equation (1):

$$\ln(c_0/c_t)=kt \quad (1)$$

where c_0 and c_t are the sulfur contents of model gasoline at time zero and time t(s), respectively, and k is the first-order rate constant(h^{-1}). Half-life ($t_{1/2}$/h was calculated *via* equation (2), which was derived from Eq.(1) by replacing c_t with $c_0/2$

$$t_{1/2}=0.693/k \quad (2)$$

Fig.6 shows the time-course variation of $\ln(c_0/c_t)$, the data of which were obtained from data shown in Fig.4. k and $t_{1/2}$ could be calculated. k and $t_{1/2}$ were 0.1694 h^{-1} and 4.09 h, respectively, when no zeoliteartificial was added. When 0.15 g of zeoliteartificial was added in the combined solution(100 mL), k and $t_{1/2}$ were changed to 0.5047 h^{-1} and 1.37 h, respectively. Here, these results strongly supported the first-order kinetics for the photo-oxidation of thiophene.

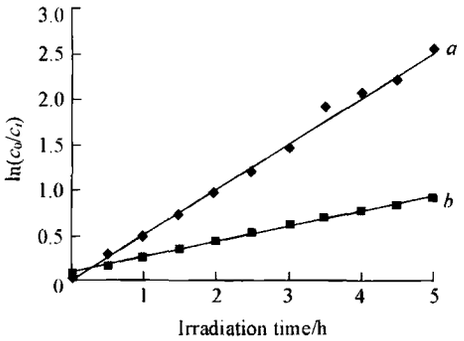

Fig.6 Time-course variation of $\ln(c_0/c_t)$

a. 0.15 g of zeoliteartificial, $y=0.5047x-0.0039$, $R=0.9954$; *b*. no zeoliteartificial, $y=0.1694x+0.0876$, $R=0.9958$.

3.5 Products of Photo-oxidation and Mechanism

In the reaction, the air out of outlet was introduced to distilled water, the pH of which was 7.06 during reaction and the pH of water after reaction was decreased to 3.52 that was nearly to the pH of saturated H_2CO_3 at 298 K(3.49). When $KMnO_4$ solution was added into the water, the color of $KMnO_4$ did not fade, which indicated that there was no SO_2 in the photo-oxidation products of thiophene. When the air out of the outlet was introduced to a clear $Ca(OH)_2$ solution, the solution became turbid. Above phenomenon indicated that CO_2 was one of the products of photo-oxidation of thiophene.

To verify the products further, water was used as the extraction solvent to replace MeCN. When $KMnO_4$ solution was dropped into the resulting water phase, the color of $KMnO_4$ faded. When $BaCl_2$ solution was added into the solution, it did not fade, and a white precipitate was formed. Above phenomenon indicated that there were SO_4^{2-} and maybe oxalic acid in the products of photo-oxidation of thiophene.

Fig.7 shows the IR spectrum of the products of photochemical oxidation of thiophene. There was an absorption peak at 1634 cm^{-1}, which was attributable to the stretching vibration of C=O bond. The peak at 2500—3000 cm^{-1} was attributable to the stretching vibration of O—H existed as dimer. And there were

also two absorption peaks at 1449 and 919 cm^{-1}, which were attributable to O—H bond. These suggest that there was —COOH contributed by oxalic acid in the products[16]. 1039 cm^{-1} was the bending vibration absorption peak of S O, which indicated the existence of thiophene sulfone.

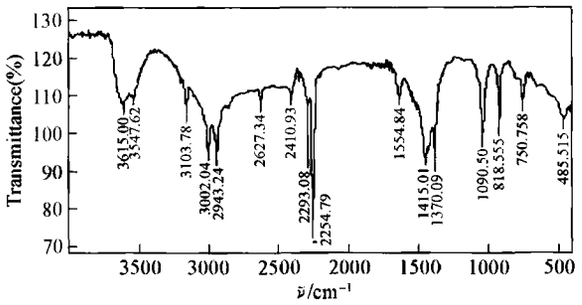

Fig.7 FTIR spectrum of photochemical oxidation products of thiophene

Canela *et al.*[17] has found that there were SO_4^{2-}, SO_2, and SO as the products of thiophene photocatalyzed by TiO_2. These were formed because of the difference between oxidant and photocatalyst.

When there was no thiophene in *n*-octane, the above phenomenon was not observed. This indicated that *n*-octane could not be oxidized by O_2 under UV light.

On the basis of the above phenomenon, the photo-oxidation mechanism of thiophene is proposed here, which is shown as follow.

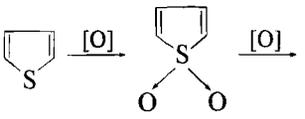

$$SO_3 + 2CO_2 + HOOCCOOH + H_2O \quad (3)$$

The detailed paths of mechanism are shown in equations (4) and (5).

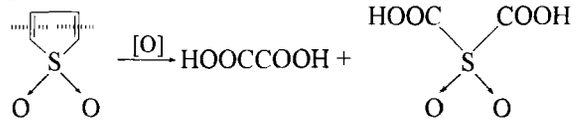

(4)

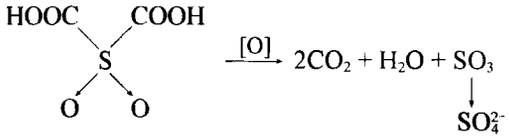

(5)

4 Conclusions

The desulfurization process of thiophene by a combination of photochemical reaction and liquid-liquid extraction has been investigated, and the following results were obtained.

(1) Thiophene dissolved in *n*-octane was successfully photodecomposed using a high-pressure mercury lamp and was removed to the water phase under the conditions of room temperature and atmospheric pressure. O_2 in air is an effective oxidant for thiophene under UV light, and desulfurization of thiophene is improved by the addition of zeoliteartificial, which is an adsorbent for O_2. Desulfurization yield of thiophene dissolved in *n*-octane was 92.3% as 0.15 g of zeoliteartificial was added after 5 h of photoirradiation.

(2) The photo-oxidation of thiophene by O_2 follow first-order kinetics, and the main photo-oxidation products of thiophene are sulfone, oxalic acid, SO_4^{2-}, and CO_2.

References

[1] Song Chun-shan, Ma Xiao-liang, *Applied Catalysis B*, **2003**, *41*(1/2), 207
[2] Matsuzawa S., Tanaka J., Sato S., *et al.*, *J. Photoch. Photobio. A*, **2002**, *149*(1—3), 183
[3] Shiraishi Y., Hirai T., Komasawa I., *Ind. Eng. Chem. Res.*, **1998**, *37*(1), 203
[4] Li Fa-tang, Zhao Di-shun, *Modern Chemical Industry*, **2005**, *25*(9), 14
[5] Wang Lei, Shen Ben-xian, Li Shu-zhen, *Energy & Fuels*, **2006**, *20*(3), 1287
[6] Shiraishi Y., Hirai T., Komasawa I., *Ind. Eng. Chem. Res.*, **2001**, *40*(1), 293
[7] Aladin I., Shen Ben-xian, Zhou Wei, *Petrol. Sci. Technol.*, **2003**, *21*(9/10), 1555
[8] Zhong Ping, Kong Ling-ren, Lin Zhi-fen, *et al.*, *Bull. Environ. Contam. Toxicol.*, **2003**, *70*(6), 1128
[9] Yang Hai-ying, *The Application of Gas Chromatography in Petrochemical Technolog*, Chemical Industry Press, Beijing, **2005**
[10] Hirai T., Shiraishi Y., Komasawa I., *J. Chem. Eng. Jap.*, **1997**, *30*(1), 173
[11] Shiraishi Y., Taki Y., Hirai T., *et al.*, *Chem. Commun.*, **1998**, (23), 2601
[12] Robertson J., Bandosz T. J., *J. Colloid Interf. Sci.*, **2006**, *299*(1), 125
[13] Zhao Di-shun, Liu Cui-wei, Ma Si-guo, *Chem. J. Chinese Universities*, **2006**, *27*(4), 692
[14] Zhao Di-shun, Li Fa-tang, Luo Qing-zhi, *et al.*, *Journal of Chemical Industry and Engineering*, **2006**, *57*(11), 2735
[15] Yan Wu-min, Zeng Yong-ping, Ju Shen-gui, *Petrochemical Technology*, **2006**, *35*(4), 310
[16] Xing Qi-yi, Xu Rui-qiu, Zhou Zheng, *Fundamental Organic Chemistry*, Higher Education Press, Beijing, **1993**
[17] Canela M. C., Alberici R. M., Sofia R. C. R., *et al.*, *Environmental Science & Technology*, **1999**, *33*(16), 2788

vide infra, to be discussed partly

Environ. Sci. Technol. **1999**, *33,* 2788−2792

Destruction of Malodorous Compounds Using Heterogeneous Photocatalysis

MARIA C. CANELA,
ROSANA M. ALBERICI,
RAQUEL C. R. SOFIA,
MARCOS N. EBERLIN, AND
WILSON F. JARDIM*

Instituto de Química, Universidade Estadual de Campinas, CP 6154, CEP 13083-970, Campinas, SP, Brazil

Photocatalytic oxidation of the sulfur-containing compounds, trimethylene sulfide (C_3H_6S), propylene sulfide (C_3H_6S), thiophene (C_4H_4S), and methyl disulfide ($C_2H_6S_2$), was carried out using an annular plug flow reactor with TiO_2 in a supported form. Formation of products and byproducts was monitored in real time using a mass spectrometry online system. Mineralization of the sulfur-containing compounds was confirmed by mass balance of CO_2 and SO_4^{2-}. Dilute contaminated atmospheres of trimethylene sulfide and propylene sulfide were completely mineralized. For thiophene and methyl disulfide, however, partial oxidation was observed, generating sulfur dioxide (SO_2) and sulfur oxide (SO) as byproducts, which were confirmed by parent ion MS/MS spectra as well as by chemical ionization. Sensory analysis showed that for trimethylene sulfide and propylene sulfide, odor intensity after TiO_2/UV treatment was below the olfactive threshold limit of the panel.

Introduction

The problem with malodorous emissions from sewage and industrial wastewater treatment plants has been largely discussed because it is a nuisance in any neighborhood (*1*). Sulfur-containing compounds such as mercaptans, organic sulfides, disulfides, and hydrogen sulfide are mainly responsible for obnoxious odors and have an extremely low odor threshold. Malodorous compounds can be associated with odors of different characteristics (fecal, rotten fish, rancid, etc.), according to their functional groups, and are readily detected by the human nose (*2, 3*). Most techniques of routine analysis are, however, unable to detect odor-causing compounds, hence, their identification is rather difficult even when using the most sophisticated analytical techniques (*4*). Therefore, sensory analysis is a very useful auxiliary and powerful tool to evaluate hedonistic characteristics of waters and atmospheres.

To control odors, there are several well-established conventional technologies, including adsorption by activated carbon, biofiltration and bioscrubbing, wet chemical scrubbing, thermal oxidation, and prevention. Each of these techniques displays a variety of advantages and disadvantages and different degrees of cost-effectiveness (*5*). Recently, heterogeneous photocatalysis using TiO_2 as catalyst and near UV light has attracted interest due to its potential application for the destruction of many pollutants (*6, 7*). Many of the available studies on TiO_2/UV photocatalysis have been centered on the destruction of volatile organic compounds (VOCs) for atmosphere remediation (*8*−*10*). However, the photocatalytic destruction of malodorous compounds has been only slightly explored in the gas phase (*11*−*13*).

In this work, we provide preliminary results to help the evaluation of possible application of the TiO_2/UV−vis photocatalytic process for the destruction of malodorous sulfur-containing compounds by monitoring online both target compounds and byproducts using a mass spectrometry system. As the final goal is to lower the compound concentration to a level below the human odor threshold limits, the efficiency of the process was also validated using sensory analysis.

Experimental Section

Titanium dioxide, which was supported in the photocatalytic reactor, as described by Alberici and Jardim (*8*), was obtained from Degussa (P-25) with an average particle diameter of 30 nm, a crystal structure of primarily anatase, and a surface area of 50 ± 15 m^2 g^{-1} (BET). The contaminated atmosphere was generated by continuously vaporizing the liquid, in synthetic air. Trimethylene sulfide, propylene sulfide, thiophene, and methyl disulfide (all provided by Aldrich) were used as received in a range of concentration between 20 and 86 ppmv, in synthetic air. Concentration values were chosen considering the background levels of these compounds in the environment and their extremely low odor threshold.

The annular photoreactor consists of a glass cylinder (3.5 cm i.d. × 86 cm height) and a 30 W black-light lamp (Sankyo Denki Japan-BLB) that serves as the inner surface of the annulus. The internal wall of the glass tube was coated with TiO_2 at a loading density of 9.5×10^{-4} g/cm^2, using a simple soaking/drying coating method. A TiO_2 film thickness of ca. 5.3 μm was estimated by the Scanning Electron Micrograph technique (SEM). The UV light intensity at the TiO_2 coating was 4.5 mW cm^{-2} measured by a Cole Parmer radiometer at 365 nm. The photoreactor was fed with synthetic air containing 21% of oxygen and 23% of relative humidity, since water vapor and oxygen are required to maintain long-term catalyst photoactivity (*14*−*17*). Experiments were performed in a single pass mode at a flow rate of 250−500 mL min^{-1}, which corresponds to a gas residence time of 1.61−0.81 min at room temperature. No mass transfer limitations were observed when this reactor was used in the destruction of many VOCs, as reported in details by Alberici and Jardim (*8*). Steady-state conditions were normally achieved after 30 min of UV-irradiation. Conversion rates were monitored using a GC-FID (SHIMADZU GC-14B gas chromatograph) equipped with a DB-624 (30 m × 0.54 mm × 3 μm J&W) fused silica megabore column. Experiments under UV irradiation, but in the absence of catalyst, were performed to evaluate conversions owing to photolysis only. A more detailed discussion of the experimental apparatus and procedures is described elsewhere (*8*).

The destruction of target compounds and the formation of byproducts during the gas-phase photocatalytic oxidation were monitored using a mass spectrometry online monitoring system and selected ion monitoring (SIM). The catalytic photoreactor outlet was connected directly to the gas inlet of an Extrel (Pittsburgh, PA) pentaquadrupole mass spec-

* Corresponding author phone/fax: +55 19 7883135; e-mail: wfjardim@iqm.unicamp.br.

10.1021/es980404f CCC: $18.00
Published on Web 07/13/1999

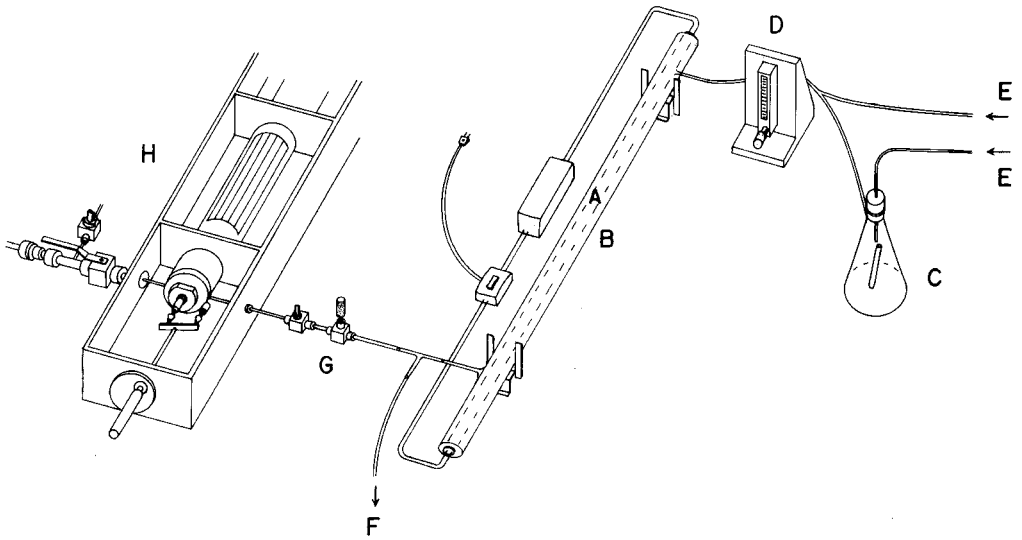

FIGURE 1. Schematic representation of the photocatalytic degradation system and the MS/MS online monitoring: A, black-light lamp; B, photoreactor; C, sulfur-containing compounds reservoir; D, flow meter; E, carrier gas; F, waste; G, needle valve flow control; and H, mass spectrometer.

trometer (*18, 19*), consisting of three mass analyzers (Q1, Q3, Q5) and two reaction quadrupoles (q2, q4). The gaseous mixture was ionized by either 70 eV electron impact (EI) or chemical ionization (CI). The pentaquadrupole mass spectrometer was also used to help identify products through collision induced dissociation (CID) of mass-selected ions in MS/MS spectrometry. The mass spectrometer is also equipped with a second inlet system, from which known amounts of calibration gases were introduced to quantify the compounds. This procedure was used for target compounds only (Figure 1).

After the photooxidation experiments, the reactor was washed six times with 50 mL of water to remove all adsorbed products. The concentration of sulfate ions was determined by turbidimetry (*20*). Sulfur dioxide was concentrated by scrubbing through sodium tetrachloromercurate(II) and subsequently determined by colorimetry using *p*-rosaniline (*21*). Carbon dioxide was monitored in the gas phase using flow injection analysis (FIA) (*22*). In this method, CO_2 diffuses through a PTFE membrane toward a deionized water stream, forming HCO_3^- and H^+ ions that continuously flow through a conductometric detector. The solution conductance is proportional to the total CO_2 concentration of the gaseous sample.

Sensory analysis was carried out with eight panelists trained to use Flavor Profile Analysis (FPA) (*20*). Panelists were carefully selected according to their sensitivities to the basic odor and had been trained to sample evaluation and description according to both the Standard Methods for the Examination of Water and Wastewater (*20*) and Damásio and Costell (*23*).

Panelists were exposed to the treated atmosphere after the TiO_2/UV and the odor intensity was compared to the initial concentration of the compounds kept in a Tedlar bag. The panelists used a flat scale of 10 cm to register the odor intensity. The flat scale is a horizontal line with two extremities, ranging from weak to strong odor intensity. The panelists score the smell in the outlet reactor after comparing the odor with odor free air and an air sample collected before irradiation. Sensory analyses were carried out only for compounds that were totally mineralized as determined by both mass balance (CO_2 and SO_4^{2-}) and MS analysis, to avoid exposing the panelist to possible hazardous compounds formed due to partial destruction of the parent compound.

Results and Discussion

Initial experiments showed that both UV light and TiO_2 were necessary to the oxidation of the sulfur-containing compounds. High levels of destruction of these compounds were measured using both the GC-FID and the mass spectrometry online monitoring system. Figure 2 displays the 70 eV mass spectra obtained before and after UV-irradiation, showing the disappearance of the target compound with concomitant generation of new signals due to byproducts. Table 1 shows further details for each peak with their respective identification, based on the National Institute of Standard (NIST) mass spectral library. In the TiO_2/UV degradation of propylene sulfide (Figure 2a) and trimethylene sulfide (Figure 2b), carbon dioxide was the only final product in the gas phase identified by MS (m/z 44). For thiophene (Figure 2c) and methyl disulfide (Figure 2d), the ions of m/z 64 and 48 are also present in the respective mass spectra. The identities of these ions were investigated using tandem mass spectrometry (MS/MS) and CID (*24*). The ion m/z 64 dissociates producing the fragments of m/z 48 and 32. Considering that m/z 64 corresponds to $SO_2^{\bullet+}$, the fragment of m/z 48 ($SO^{\bullet+}$) is generated by O loss and the fragment of m/z 32 ($S^{\bullet+}$) by either O loss from $SO^{\bullet+}$ (*25*) or O_2 loss from $SO_2^{\bullet+}$. Because the fragment of m/z 48 also dissociates to m/z 32, it is not possible to determine whether the ion of m/z 48 results from dissociation of $SO_2^{\bullet+}$ (m/z 64) or direct ionization of SO. However, thiophene photodegradation experiments monitored by chemical ionization mass spectrometry (Figure 3) proved that the ionic fragment of m/z 48 is formed directly from neutral SO. Before UV-irradiation, only protonated thiophene (m/z 85) is observed in the CI mass spectrum (Figure 3a). After partial photodegradation (Figure 3b), signals corresponding to protonated SO_2 (SO_2H^+) of m/z 65 and protonated SO (SOH^+) of m/z 49 are also detected. Note that no dissociation of SO_2H^+ to SOH^+ is expected due to the mild chemical ionization conditions and the highly unfavorable O loss from the closed-shell ion SO_2H^+. For methyl disulfide however, EI-MS monitoring showed that only SO_2 is produced (spectra not shown).

Figure 4 shows the MS-SIM profile of the online monitoring of TiO_2/UV degradation of methyl disulfide (Figure 4a), thiophene (Figure 4b), propylene sulfide (Figure 4c), and trimethylene sulfide (Figure 4d). As the UV light is turned on, the concentration of the sulfur-containing compounds

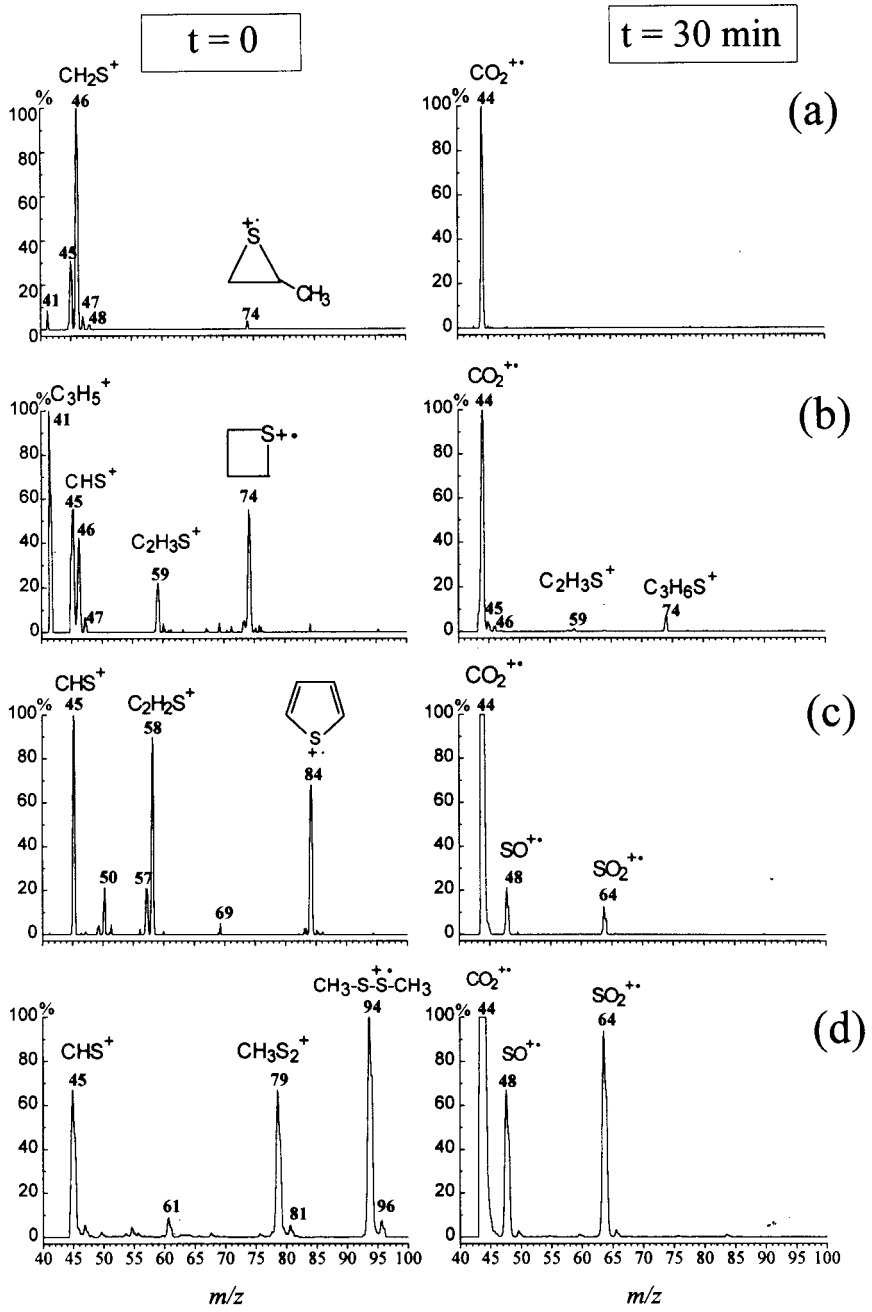

FIGURE 2. EI mass spectra (70 eV) of the gaseous synthetic air mixture containing (a) propylene sulfide, (b) trimethylene sulfide, (c) thiophene, and (d) methyl disulfide compounds before and after 30 min of UV-irradiation. Experimental conditions: 30 W black-light lamp, 21% oxygen, and 23% relative humidity.

decreases rapidly with the concomitant generation of carbon dioxide. The ions of m/z 48 and 64 have also been used to monitor the photodegradation of methyl disulfide (Figure 4a) and thiophene (Figure 4b). Note that in Figure 4a, $SO^{\bullet+}$ is produced mainly from dissociation of the $SO_2^{\bullet+}$ ion, whereas in Figure 4b, $SO^{\bullet+}$ corresponds both to dissociation of $SO_2^{\bullet+}$ and direct ionization of SO.

Table 2 summarizes the results obtained in the gas-phase photocatalytic destruction of all four sulfur-containing compounds under optimized conditions. High conversion yields (>99%) were obtained for propylene sulfide and trimethylene sulfide, with complete mineralization to CO_2 and SO_4^{2-}, as shown by carbon and sulfur mass balance. In the photodegradation of methyl disulfide and thiophene, SO_2 was detected as an additional byproduct. For methyl disulfide, 100% sulfur mass balance was achieved. For thiophene, however, sulfur mass balance reached 88% only, and this low sulfur yield can be attributed to SO formation (not quantified), as demonstrated by the CI-MS analysis. For methyl disulfide and thiophene, CO_2 could not be quantified due to the interference of SO_2 in the Conductometry-Flow Injection-Analysis (FIA). Sulfur dioxide also diffuses through the PTFE, yielding conductance signals.

Although there are very few papers on the literature dealing with the destruction of sulfur-containing compounds using the photocatalytic process, recently, Peral and Ollis (*26*) using TiO_2/UV process obtained 10% conversion in the destruction of the dimethyl sulfide. The authors did not detect any sulfur compound on the TiO_2, which was attributed to either the formation of SO_2 or SO_3 or to the formation of another mercaptan. Suzuki (*12*), using a honeycomb type of gaseous reactor, found that the destruction rates of S-compounds (CH_3SH and H_2S) were in the range of 0.13 min^{-1}.

TABLE 1. Major Ions in the 70 eV EI Mass Spectra of Sulfur Containing Compounds

Precursor	Name	*m/z* (relative abundance)
	trimethylene sulfide	41 (100), 45 (53), 46 (39), 47 (7), 59 (21), 74 (53)
	propylene sulfide	41 (8), 45 (35), 46 (100) 47 (5), 48 (3), 74 (3)
CH_3-S-S-CH	methyl disulfide	45 (67), 61 (10), 79 (67), 81 (5), 94 (100), 96 (10)
	thiophene	45 (100), 50 (20), 57 (20), 58 (91), 69 (6), 84 (69)
SO_2	sulfur dioxide	32 (11), 48 (50), 64 (100)
SO	sulfur oxide	32 (20) 48 (100)

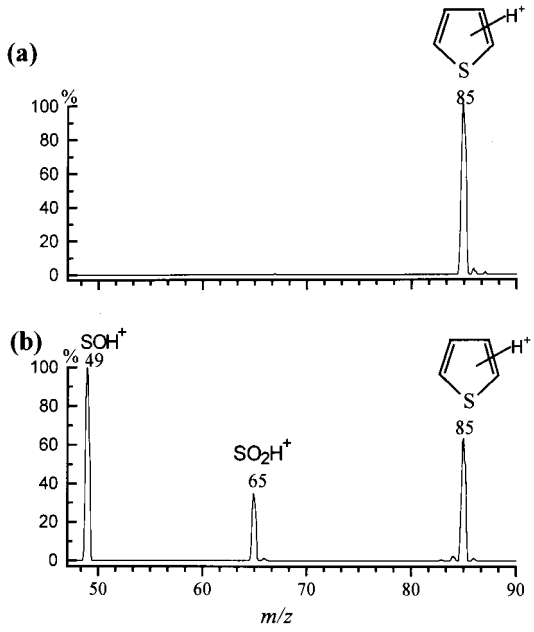

FIGURE 3. Methane-CI mass spectra of TiO_2/UV degradation of thiophene (a) before and (b) during UV-irradiation.

The general equations for the complete photocatalytic conversion of sulfur-containing compounds may be described by the following stoichimetry

$$C_xH_yS_z + (4x+6z+y)/4O_2 \rightarrow xCO_2 + 2zH^+ + zSO_4^{2-} + (y-z)/2H_2O \quad (1)$$

and could be applied to trimethylene sulfide and propylene, but for thiophene and methyl disulfide, the formation of SO_2 and SO as byproducts altered the reaction stoichimetry. For 1 mol of thiophene, 0.82 mol of sulfate ions, 0.06 mol of sulfur dioxide, and 0.12 mol of sulfur oxide were generated. For 1 mol of methyl disulfide however, 1.53 mol of sulfate ions and 0.47 mol of sulfur dioxide were generated.

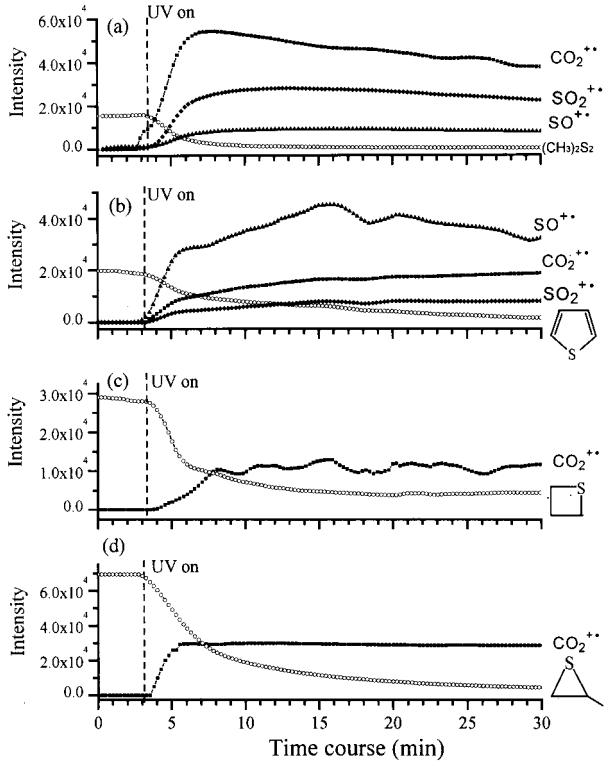

FIGURE 4. Diagrams of SIM-MS monitoring of TiO_2/UV degradation of methyl disulfide (a), thiophene (b), propylene sulfide (c), and trimethylene sulfide (d): (○) target compounds, (■) *m/z* 44 ($CO_2^{\bullet+}$), (▲) *m/z* 48 ($SO^{\bullet+}$), and (◆) *m/z* 64 ($SO_2^{\bullet+}$). Dashed lines indicate the time when the reactor was turned on.

SCHEME 1

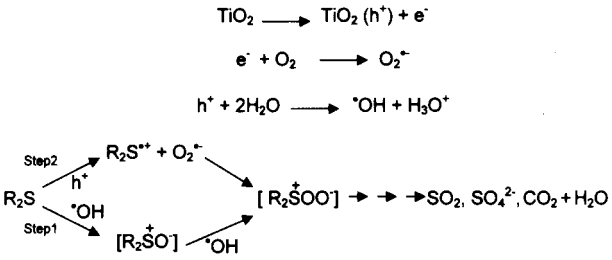

The formation of different radicals from the illumination of TiO_2 in water is well established in the literature (*6*). Both positive holes and hydroxyl radicals have been proposed as the oxidizing species responsible for initiating the attack on organic solutes. In Scheme 1 we show a proposed mechanism with the parallel reaction paths for both positive holes and hydroxyl radicals. When photocatalytic oxidation is conducted in the presence of water, the primary product of the electron transfer is often an adsorbed hydroxyl radical (step

TABLE 2. Initial Conditions and Sulfur-Containing Compounds Degradation Rates

substrate	C_{inlet} (ppmv)	res. time (min)	flow (mL/min)	conv (%)	oxid rate (μmol/min)	SO_4^{2-} rate (μmol/min)	SO_2 rate (μmol/min)	CO_2 rate (μmol/min)	sulfur balance (%)	carbon balance (%)
trimethylene sulfide	61	1.81	262	99	0.72	0.71	nd	2.16	99	100
propylene sulfide	86	0.99	409	99	1.58	1.58	nd	4.65	100	98
thiophene	54	1.30	324	99	0.79	0.65	0.05	*a*	88	*a*
methyl disulfide	34	0.85	474	99	0.72	0.55	0.17	*a*	100	*a*

[a] CO_2 analysis was not carried out due to SO_2 interference in the Conductometry-Flow Injection-Analysis (FIA).

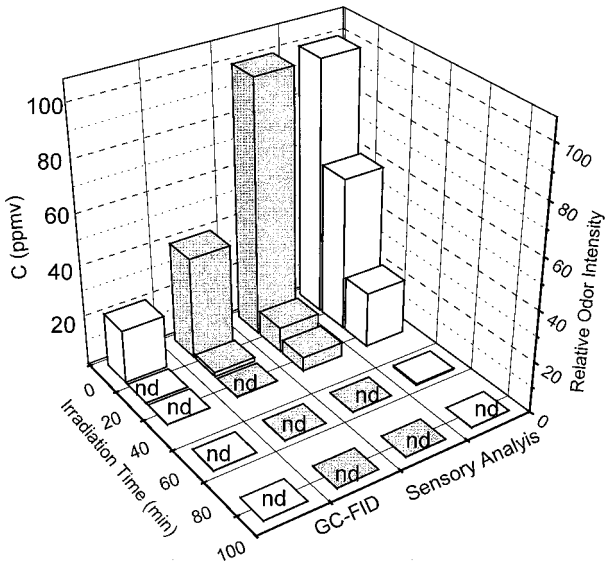

FIGURE 5. Performance of the TiO_2/UV process in the destruction of propylene sulfide (white) and trimethylene sulfide (black) as monitored by GC-FID and sensory analysis: nd = not detectable.

1). Long known for its high reactivity, this species can attack the sulfur-containing organic compounds generating the oxidation products as sulfoxides and sulfones. In another way (step 2), the photogenerated hole localized at the surface of the irradiated semiconductor is trapped by an adsorbed sulfur-containing organic compound, generating an adsorbed cation radical. The formation of a sulfur radical cation has been previously reported by Davidson and Pratt (*27*) and Fox and Abdel-Wahab (*28, 29*) in the presence of oxidatively inert solvents. In the experimental conditions used in this work it was not possible to detect either sulfoxides or sulfones (intermediates) because gas-phase reactions are very fast, generating as final products SO_2 and SO_4^{2-} as shown by the mass balance.

Although sulfate ions formed during the photocatalytic process were adsorbed onto the catalyst surface, no catalytic deactivation was observed in these experiments. Using H_2S, Canela et al. (*13*) showed that sulfate ions adsorbed onto TiO_2 promoted a decrease in the photocatalytic activity when high concentrations of H_2S (600 ppmv; corresponding to 5.4 μmol min^{-1} of SO_4^{2-}) were used. However, at 217 ppmv (1.9 μmol min^{-1} of SO_4^{2-}) of H_2S, the photocatalytic activity was maintained for 24 h of continuous use. For all the sulfur-containing compounds tested in the present work, the maximum sulfate ions load observed was 1.58 μmol min^{-1}, as shown in Table 2.

A comparative performance of the analytical technique used to monitor the target compounds (GC-FID) versus the sensory analysis is shown in Figure 5. Both GC-FID and sensory analysis indicate that the photocatalytic process was efficient to destroy the malodorous compounds. The panelists were unable to detect odor for both methylene sulfide and propylene sulfide in the outlet reactor, within 60 min after of the irradiation. On the other hand, using chromatographic analysis, after 15 min, it was not possible to detect the target compound in the outlet reactor. This result emphasizes the importance of sensory analysis in the evaluation process of destruction of malodorous compounds.

Acknowledgments

Financial support from the Fundação de Amparo à Pesquisa do Estado de São Paulo (FAPESP) (Grants 97/01545-6, 97/00758-6, 95/9497-5, and 97/6172-3) and the Conselho Nacional de Desenvolvimento Cientifico e Tecnológico (CNPq) are greatly acknowledged.

Literature Cited

(1) Lutz, M.; Davidson, S.; Stowe, D. *Water Environ. Technol.* **1995**, *6*, 52−57.
(2) Bonnin, C.; Laborie, A.; Paillard H. *Water Sci. Technol.* **1990**, *22*, 65−74.
(3) Hwang, Y.; Matsuo, T.; Hanaki, K.; Suzuki, N. *Water Res.* **1995**, *29*, 711−718.
(4) Young, W. F.; Horth, H.; Crane, R.; Ogden, T.; Arnott, M. *Water Res.* **1996**, *30*, 331−340.
(5) Mills, B. *Filtration Separation* **1995**, *02*, 147−152.
(6) Hoffman, M. R.; Martin, S. T.; Choi, W.; Bahnemann, D. W. *Chem. Rev.* **1995**, *95*, 69−96.
(7) Mills, A.; Hunte, S. L. *J. Photochem. Photobiol., A* **1997**, *108*, 1−35.
(8) Alberici, R. M.; Jardim, W. F. *Appl. Catal., B* **1997**, *14*, 55−68.
(9) Dibble, L. A.; Raupp, G. B. *Environ. Sci. Technol.* **1992**, *26*, 492−495.
(10) Peral, J.; Ollis, D. F. *J. Catal.* **1992**, *136*, 554−565.
(11) Suzuki, K.; Satoh, S.; Yoshida, T. *Denki Kagaku* **1991**, *59*, 521−523.
(12) Suzuki, K. In *Photocatalytic Air Purification on TiO_2 Coated Honeycomb Support*; Ollis, D. F., Al-Ekabi, H., Eds.; Elsevier: Amsterdan; 1993; Photocatalytic Purification and Treatment of Water and Air, Vol. 3, p 421.
(13) Canela, M. C.; Alberici, R. M.; Jardim, W. F. *J. Photochem. Photobiol., A* **1998**, *112*, 73−80.
(14) Lu, G.; Linsebigler, A. L.; Yates, J. T., Jr. *J. Phys. Chem.* **1995**, *99*, 7626−7631.
(15) Lu, G.; Linsebigler, A. L.; Yates, J. T., Jr. *J. Chem. Phys.* **1995**, *102*, 4657−4662.
(16) Raupp, G. B.; Junio, C. T. *Appl. Surf. Sci.* **1993**, *72*, 321−327.
(17) Wong, J. C. S.; Linsebigler, A. L.; Lu, G.; Fan, J.; Yates, J. T., Jr. *J. Phys. Chem.* **1995**, *99*, 335−344.
(18) Juliano, V. F.; Gozzo, F. C.; Eberlin, M. N.; Kascheres, C. *Anal. Chem.* **1996**, *68*, 1328−1334.
(19) Eberlin M. N. *Mass Spectrom. Rev.* **1997**, *16*, 113−144.
(20) *Standard Methods for the Examination of Water and Wastewater*, 18th ed.; Greenberg, A. S., Clesceri, I. S., Eaton, A. D., Eds.; American Public Health Association: Washington, DC, 2.19−2.23 (section 2170, Flavor Profile Analysis), 4.126−4.132 (4500-SO_4^{2-}), 1992.
(21) West, P. W.; Gaeke, G. C. *Anal. Chem.* **1956**, *28*, 1816−1819.
(22) Jardim, W. F.; Guimarães, J. R.; Allen, H. E. *Ciência Cultura* **1991**, *43*, 454−456.
(23) Damásio, M. H.; Costell, E. *Rev. Agroquím. Tecnol. Aliment.* **1991**, *31*, 165−178.
(24) Bush, K. L.; Glish, G. L.; McLuckey, S. A. *Mass Spectrometry/Mass Spectrometry Techniques and Applications of Tandem Mass Spectrometry*; VCH Publishers: 1989.
(25) Sparrapan, R.; Mendes, M. A.; Ferreira, I. P. P.; Eberlin, M. N.; Santos, C.; Nogueira, J. C. *J. Phys. Chem. A.* **1998**, *102*, 5189−5195.
(26) Peral, J.; Ollis, D. F. *J. Mol. Catal. A* **1997**, *115*, 347−354.
(27) Davidson, R. S.; Pratt, J. E. *Tetrahedron Lett.* **1983**, *24*, 5903−5906.
(28) Fox, M. A.; Abdel-Wahab, A. A. *Tetrahedron Lett.* **1990**, *31*, 4533−4536.
(29) Fox, M. A.; Abdel-Wahab, A. A. *J. Catal.* **1990**, *126*, 693−696.

Received for review April 20, 1998. Revised manuscript received April 30, 1999. Accepted May 20, 1999.

ES980404F